

Revealing the spin optics in conic-shaped metasurfaces

Yanjun Bao, Shuai Zu, Wei Liu, Xing Zhu, and Zheyu Fang*

School of Physics, State Key Lab for Mesoscopic Physics, Peking University, Beijing 100871, China

(Received)

e-mail address: zhyfang@pku.edu.cn

Ellipse and hyperbola are two old curves in mathematics and have found their applications in various fields. Here, we investigate the peculiar optical spin properties of the two curves and establish a connection between their foci and the spin states of incident light. We show that optical spin Hall effect (OSHE) can exist in an ellipse-shaped metasurface, where photons with different spin states can be exactly separated to each of its two foci. For a hyperbola-shaped metasurface, optical spin-selective effect is observed that only photons with one certain spin state can be accumulated at its foci. We apply these concepts to design spin-based plasmonic devices with various functionalities. We believe that our configuration may provide a route for spin-based plasmonic device design and open up a new realm for the application of traditional conic sections.

DOI:

PACS: 07.79.Fc, 42.25.-p, 42.25.Ja, 42.79.-e, 73.20.Mf

Light transports with two distinct forms of angular momentum, respectively named orbital angular momentum (OAM) and spin angular momentum (SAM) [1]. Recently, a new branch of optical field, spin optics, has emerged and attracted considerable attention. This field concerns the spin-dependent optical phenomena, such as optical spin Hall effect (OSHE) [2-4], where the spin degeneracy of photons is removed through spin-orbit interaction, spin-dependent plasmonic focusing lens [5], spin-dependent optical vortex [6, 7], et al. On the other hand, metasurfaces, artificially subwavelength-structured interfaces, are able to control the phase of light, leading to versatile optical functionalities [8-11]. The use of metasurfaces in spin optics provides a flexible platform and an additional degree of freedom for applications of OSHE [12, 13], optical Rashba effect [14] and holography [15-18].

Ellipse and hyperbola are two curves that are common in physics, astronomy and engineering. The two foci are two special points in the determination of their geometric curves and give rise to many unique properties. For example, light emanating from a focus of an elliptical mirror can be reflected by the elliptical structure and propagates into the second one, and for a hyperbolic mirror, light directed towards at a focus can be reflected to the other one. The reflective properties of the two curves are used in the design of whisper gallery, radio telescopes and some optical telescopes. However, the optical spin properties of the two conic-shaped structures have never been investigated and how their foci connect with the incident spin states remains mysterious.

Here, for the first time, we investigate and reveal the difference of the spin optical properties between elliptical and hyperbolic curves. Nanoslits as the scattering element

are arranged on the elliptical and hyperbolic traces. Facilitated by the spin-dependent geometric phase of nanoslit, OSHE and spin-selective effect are observed in ellipse-shaped and hyperbola-shaped metasurfaces, respectively. The foci of the two conic curves are demonstrated to have a strong connection with both

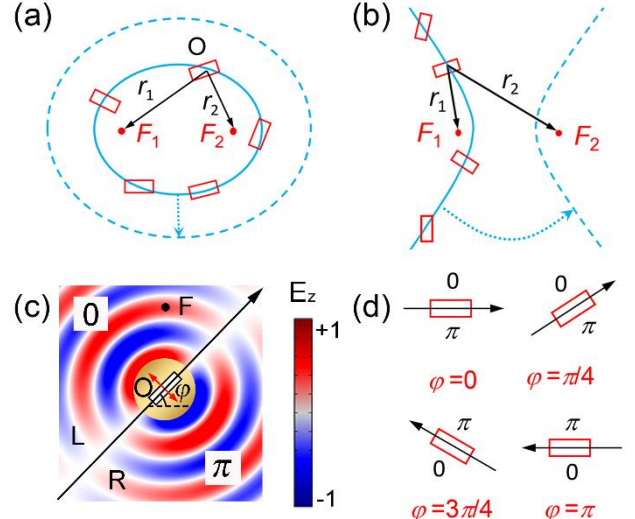


Fig. 1 (color online). (a-b) Schematic of ellipse (a) and hyperbola (b) with nanoslits located on their traces. (c) Calculated normal component of the SPP electric field E_z launched by a nanoslit with an azimuthal angle φ that is perforated in an Au film when the incident light is polarized perpendicular to its long axis (polarization indicated by a red arrow). (d) Anti-phase distributions of four nanoslits with different azimuthal angles.

phenomena. These concepts are verified experimentally by using scanning near-field optical microscopy (SNOM). Furthermore, the spin optical properties of the conic curves are utilized to design spin-based plasmonic devices with various functionalities.

As shown in Fig. 1(a), the trace of ellipse is determined by $r_1+r_2=const.$, where r_1 and r_2 are the distances from any point at the ellipse to the two foci F_1 and F_2 , respectively. Instead of corrugating an ellipse-shaped slit in metallic film [19], we arrange nanoslits with different azimuthal angles that are perforated in Au film at the elliptic trace. This angle provides us an extra degree of freedom to control photons with different spin states [12, 20]. Interestingly, we found that with proper azimuthal angles of nanoslits, photons with different spin states can be exactly separated to each of the two foci of ellipse, which can be regarded as OSHE.

To prove the OSHE and determine the azimuthal angle of each nanoslit, we firstly consider the surface plasmon polaritons (SPPs) excited by a nanoslit O perforated in an Au film, as shown in Fig. 1(c). The black arrow indicates the direction of its long axis with an azimuthal angle φ , which is limited between 0 to π because the same nanoslit can be obtained if it is rotated by π . SPPs are preferentially generated when the normal incident light is polarized perpendicular to its long axis. The SPP emission is approximately that of an in-plane point dipole and exhibits an anti-phase pattern relative to the long axis of nanoslit [21]. We define this anti-phase $\psi(O,F)=0$ if a point F is located at the left-hand-side of the directional vector of nanoslit (back arrow) and π otherwise. Figure 1(d) shows this anti-phase distributions for several cases with different azimuthal angles. Noticeably, the phase patterns are totally opposite for the two cases with $\varphi=0$ and π , although they are indeed the same. This contradiction can be explained by including the geometric phase, which will be introduced below.

When the structure was illuminated by circularly polarized (CP) light which is denoted with a spin state $|\sigma_{\pm}\rangle$, an additional geometric phase $\psi_g=\sigma\varphi$ is added due to the spin-orbit interaction [22], where $\sigma=\pm 1$ corresponds to the incident spin state $|\sigma_{\pm}\rangle$. The initial phase of nanoslit is then $\psi_i=\sigma\varphi+\psi(O,F)$. Thus nanoslit can launch SPPs with different initial phase by varying its azimuthal angle. Here, we can see that the initial-phase distributions are the same for the two nanoslits with $\varphi=0$ and π . Because the angle φ can vary from 0 to π , ψ_i can cover the full range of 2π phase. However, for a fixed point F and nanoslit, the initial-phase range is limited. For example, the point F is always located at the same side of a nanoslit if they both lie on the x axis and thus can only cover π phase range.

With these in mind, we can demonstrate the existence of OSHE in ellipse-shaped metasurface. To make sure that photons with different spin states can be exactly focused at each of the two foci of ellipse, we have the following

constructive conditions for all nanoslits: $-\varphi+\psi(O,F_1)+2\pi r_1/\lambda_{\text{spp}}=2\pi m+\varphi_1$ for $|\sigma_{-}\rangle$ illumination at point F_1 and $\varphi+\psi(O,F_2)+2\pi r_2/\lambda_{\text{spp}}=2\pi n+\varphi_2$ for $|\sigma_{+}\rangle$ illumination at point F_2 . The three terms on the left side of both equations are geometric phase, anti-phase and phase retardation of SPPs from O to the two foci, respectively. By adding the two equations above, we have $r_1+r_2=(k/2+\varphi_0)\lambda_{\text{spp}}$ [23], where m , n and k are integers, φ_0 , φ_1 and φ_2 are constant values and λ_{spp} is the SPP wavelength. It is clear to see that the nanoslits are located at the elliptic trace. The angle of each nanoslit is not arbitrary but accurately determined by either equation of the two constructive equations. Similarly, we found that nanoslits located at hyperbolic traces can act as an optical spin-selective device, that only photons with one certain spin state can be accumulated at its foci. This can be easily understood by subtracting the two constructive conditions at the two foci from each other [23]. It is worth to mention that a transverse shift of the focal spots via a surface plasmon nanostructure have been observed in Ref. [22]. However, our idea differentiates it in several aspects: firstly, our structure composes of nanoslits arranged on elliptical trace, while a semicircular slit is used in Ref. [22]. Secondly, the constructive interferences at the foci of ellipse are accurate and strict, while, the foci observed in Ref. [22] is approximate and not strict, because there exist no such a

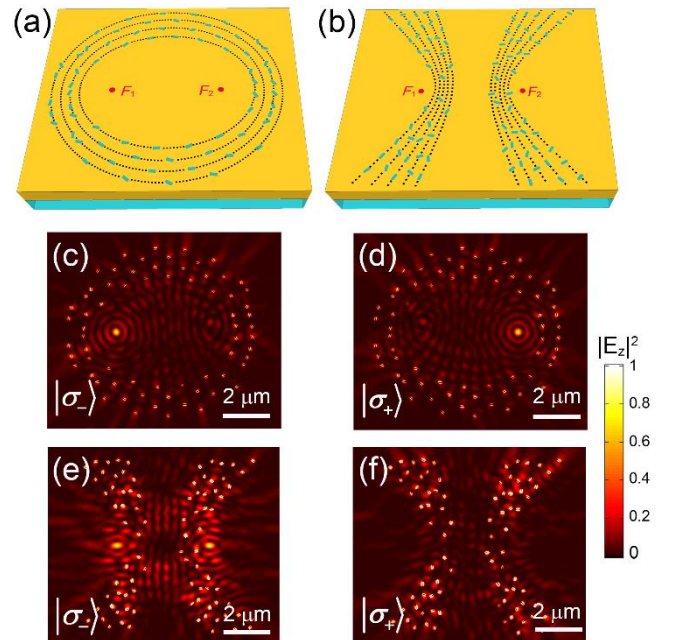


Fig. 2 (color online). (a-b) Schematics of an ellipse-shaped (a) and hyperbola-shaped (b) metasurfaces. (c-f) FDTD simulated near-field intensity $|E_z|^2$ of the ellipse-shaped (c-d) and hyperbola-shaped (e-f) metasurfaces with $|\sigma_{\pm}\rangle$ illuminations. The spin states of incident photons are indicated in each panel.

focus where all the segments of a semicircular slit can constructively interfere under CP light [23]. Finally, and the most importantly, we establish a relation between the foci of conic and incident spin states, showing that the two foci are not just two points that determine the curve traces, but indeed have its physical meanings in spin optics.

Figure 2(a) shows our designed ellipse-shaped metasurface with four elliptic traces that are etched on a 100 nm-thickness Au film. The hyperbola-shaped metasurface shown in Fig. 2(b) consists of ten hyperbolic traces [23]. The black dashed lines are drawn for the eye guide of each traces. For each trace of conic, the nanoslits at different positions have different azimuthal angles and are not fully distributed. This is because, on one hand, there is a restriction of a minimum gap of 300 nm between two adjacent nanoslits to avoid structural overlapping, and on the other hand the initial phase of nanoslit cannot cover the full range of 2π phase for a fixed point. Both structures were designed for operation at wavelength of $\lambda=671$ nm. Finite-difference time-domain

(FDTD) simulations were performed and the simulated $|\mathbf{E}_z|^2$ fields for $|\sigma_{\pm}\rangle$ incidences are shown in Fig. 2(c) and 2(d) for ellipse-shaped metasurface and in Fig. 2(e) and 2(f) for hyperbola-shaped metasurface. The simulated results show that the photons with different spin states are able to be separated to each of the elliptic foci, which is a clear demonstrating of OSHE. While for hyperbola-shaped metasurface, only photons with $|\sigma_{-}\rangle$ spin state can be focused at its both foci.

To experimentally demonstrate the concept, we fabricated the conic-shaped metasurfaces by using Au electron-beam evaporation and focused ion-beam milling [23]. Figure 3(a) and 3(b) present a scanning electron microscopy (SEM) image of the fabricated ellipse-shaped and hyperbola-shaped metasurfaces. A collection-mode SNOM system was used to measure SPP distributions. A probe with a large half-cone angle ($\approx 15^\circ$) is chosen and modified with sharp perturbation to increase the coupling efficiency of the \mathbf{E}_z component [24]. The samples were back-illuminated with circular polarized light, which is generated by a quarter wave plate and a polarizer. Figure 3(c) and 3(d) show the measured near-field optical distribution of the ellipse-shaped metasurface, which clearly demonstrate that photons with $|\sigma_{-}\rangle$ spin state are focused at F_1 , and switched to the right focus F_2 when the incident spin state is altered. For the hyperbola-shaped metasurface, only the photons with $|\sigma_{-}\rangle$ spin state can be accumulated at its both foci, as shown in Fig. 3(e) and 3(f). We note that there are some deviations between the simulation and experimental results, which may be arisen from the fabrication error, measurement accuracy and the affection of the in-plane electric field component.

As for practice applications, many structures with spin-dependent functionalities have been designed in the literature. For example, photons with different spin states can be delivered to different positions that are located at the same side [25] or each side [26] of a metasurface structure. In these structures, different functionalities require different design strategies. However, all these functionalities can be realized based on our conic-shaped metasurfaces without further design consideration. Take the ellipse-shaped metasurface for example, as shown in Fig. 4(a), points F_1 and F_2 are the common foci of the ellipses (dashed black lines) where nanoslits are located. By choosing parts of the elliptical traces, for example, regions between two foci (red rectangle) or below (green rectangle), the resulting metasurface can focus photons with opposite spin states at each side of it or at the same (upper) side. We fabricated the two metasurfaces with their SEM images shown in Fig. 4(b) and 4(c). The measured SPP intensities with $|\sigma_{\pm}\rangle$ illuminations for the two metasurfaces are shown in Fig. 3(d)-3(g), which are in good agreements with our prediction and FDTD simulated results [23]. Actually, the positions of the two foci are not

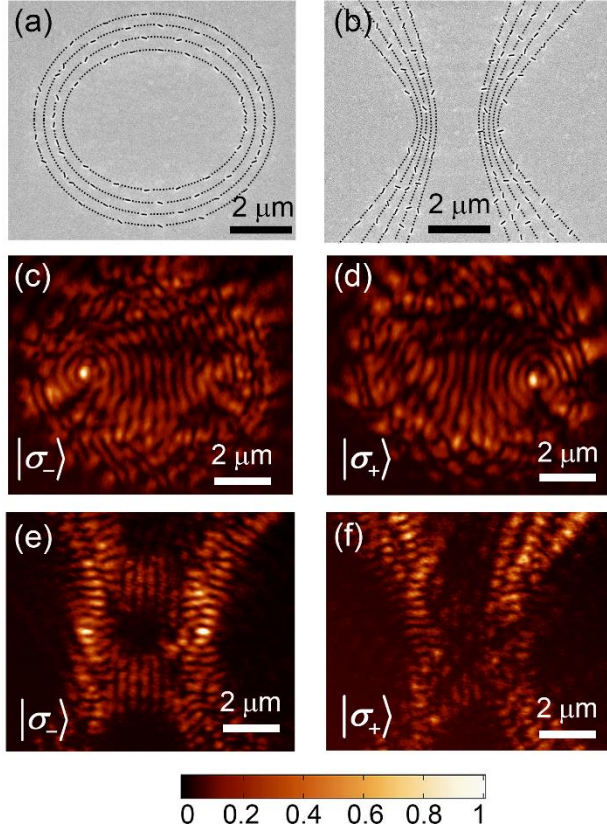


Fig. 3 (color online). (a-b) SEM images of the ellipse-shaped (a) and hyperbola-shaped (d) metasurfaces. The black dashed lines are a guide for the eye of conic traces. (c-f) Measured near-field optical intensity profiles of the ellipse-shaped (c-d) and hyperbola-shaped (e-f) metasurfaces with $|\sigma_{\pm}\rangle$ illuminations. The spin states of incident photons are indicated in each panel.

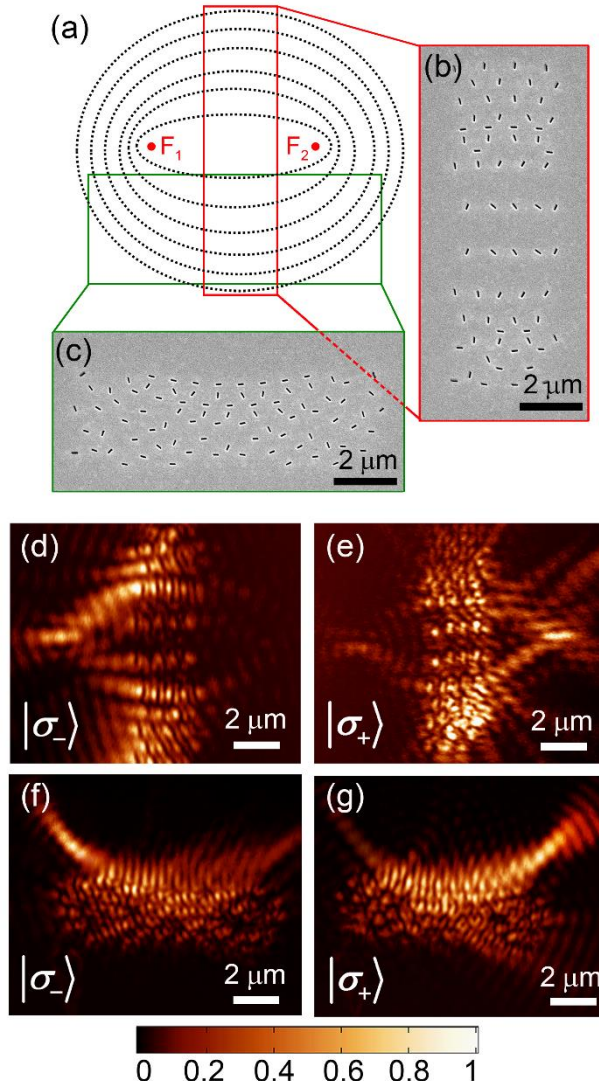


Fig. 4 (color online). (a) Design strategy of metasurfaces with different functionalities. (b-c) SEM images of two metasurfaces, which can focus photons with opposite spin states at each side of it (b) or at the same (upper) side (c). (d-g) Measured near-field optical intensities for metasurfaces shown in b (upper row) and c (lower row) with $|\sigma_{\pm}\rangle$ illuminations. The spin states of incident photons are indicated in each panel.

limited to the two cases, but can be located at arbitrary positions relative to the metasurface [23]. Similarly, if hyperbolic curve is used, two foci can be simultaneously obtained at any two points relative to the position of metasurface with CP light. The conic-shaped metasurfaces provide a fast and flexible platform for designing spin-based devices.

In summary, we investigate and experimentally demonstrate the peculiar spin optical properties of two conic curves. We show that the two curves are not only different

in their geometries, but also in the spin properties. OSHE and spin-selective effect can be observed in ellipse-shaped and hyperbola-shaped metasurfaces with a strong connection with their foci, respectively. The concept presented here opens up a new realm for the application of traditional conic sections and can be used for integrated spin-optical devices.

This work is supported by National Science Foundation of China (Grant No. 61422501, 11374023, and 61521004), the National Basic Research Program of China (973 Program, Grant No. 2015CB932403), Beijing Natural Science Foundation (Grant No. L140007), and Foundation for the Author of National Excellent Doctoral Dissertation of PR China (Grant No.2014420), and National Program for Support of Top-notch Young Professionals.

- [1] F. J. Belinfante, *Physica* **7**, 449 (1940).
- [2] N. Shitrit, I. Bretner, Y. Gorodetski, V. Kleiner, and E. Hasman, *Nano Lett.* **11**, 2038 (2011).
- [3] C. Leyder, M. Romanelli, J. P. Karr, E. Giacobino, T. C. H. Liew, M. M. Glazov, A. V. Kavokin, G. Malpuech, and A. Bramati, *Nat. Phys.* **3**, 628 (2007).
- [4] A. Kavokin, G. Malpuech, and M. Glazov, *Phys. Rev. Lett.* **95**, 136601 (2005).
- [5] X. Chen *et al.*, *Nat. Commun.* **3**, 1198 (2012).
- [6] L. Huang, X. Chen, H. Muhlenbernd, G. Li, B. Bai, Q. Tan, G. Jin, T. Zentgraf, and S. Zhang, *Nano Lett.* **12**, 5750 (2012).
- [7] E. Karimi, S. A. Schulz, I. De Leon, H. Qassim, J. Upham, and R. W. Boyd, *Light-Science & Applications* **3**, e167 (2014).
- [8] Y. J. Bao, S. Zu, Y. F. Zhang, and Z. Y. Fang, *ACS Photonics* **2**, 1135 (2015).
- [9] S. Sun *et al.*, *Nano Lett.* **12**, 6223 (2012).
- [10] N. Yu and F. Capasso, *Nat. Mater.* **13**, 139 (2014).
- [11] N. Yu, P. Genevet, M. A. Kats, F. Aieta, J. P. Tetienne, F. Capasso, and Z. Gaburro, *Science* **334**, 333 (2011).
- [12] S. Xiao, F. Zhong, H. Liu, S. Zhu, and J. Li, *Nat. Commun.* **6**, 8360 (2015).
- [13] X. B. Yin, Z. L. Ye, J. Rho, Y. Wang, and X. Zhang, *Science* **339**, 1405 (2013).
- [14] N. Shitrit, I. Yulevich, E. Maguid, D. Ozeri, D. Veksler, V. Kleiner, and E. Hasman, *Science* **340**, 724 (2013).
- [15] L. Huang *et al.*, *Nat. Commun.* **4**, 2808 (2013).
- [16] G. Zheng, H. Muhlenbernd, M. Kenney, G. Li, T. Zentgraf, and S. Zhang, *Nat. Nanotechnol.* **10**, 308 (2015).
- [17] X. J. Ni, A. V. Kildishev, and V. M. Shalaev, *Nat. Commun.* **4**, 2807 (2013).
- [18] D. D. Wen *et al.*, *Nat. Commun.* **6**, 8241 (2015).
- [19] G. M. Lerman, A. Yanai, N. Ben-Yosef, and U. Levy, *Opt. Express* **18**, 10871 (2010).
- [20] J. Lin, J. P. Mueller, Q. Wang, G. Yuan, N. Antoniou, X. C. Yuan, and F. Capasso, *Science* **340**, 331 (2013).
- [21] T. Tanemura, K. C. Balram, D. S. Ly-Gagnon, P. Wahl, J. S. White, M. L. Brongersma, and D. A. Miller, *Nano Lett.* **11**, 2693 (2011).

- [22] K. Y. Bliokh, Y. Gorodetski, V. Kleiner, and E. Hasman, Phys. Rev. Lett. **101**, 030404 (2008).
- [23] See Supplemental Material at <http://link.aps.org/supplemental/xxx> for more discussions about ellipse-shaped and hyperbola-shaped metasurfaces, the focusing of semicircular slit under CP light, the design of metasurfaces, the simulation results for Fig. 4, the focus positions of ellipse-shaped metasurfaces, the sample fabrication and optical measurements.
- [24] G. M. Lerman, A. Yanai, and U. Levy, Nano Lett. **9**, 2139 (2009).
- [25] S. Y. Lee, K. Kim, G. Y. Lee, and B. Lee, Opt. Express **23**, 15598 (2015).
- [26] X. Q. Zhang *et al.*, Adv. Mater. **27**, 7123 (2015).

Supporting Information For

Revealing the spin optics in conic-shaped metasurfaces

Yanjun Bao, Shuai Zu, Wei Liu, Xing Zhu, and Zheyu Fang^{*}

School of Physics, State Key Lab for Mesoscopic Physics, Peking University, Beijing 100871, China

*Email: zhyfang@pku.edu.cn

Contents:

- 1. Demonstration of ellipse-shaped and hyperbola-shaped metasurface for spin optics.**
- 2. Discussion of the focusing of semicircular slit with circular polarization lights**
- 3. The design of metasurfaces, sample fabrication and optical measurements.**
- 4. Simulation results of the metasurfaces shown in Fig. 4**
- 5. Focusing the photons at arbitrary positions relative the metasurfaces**

1. Demonstration of ellipse-shaped and hyperbola-shaped metasurface for spin optics.

We assume that photons with different spin states can be exactly focused at each of the two foci of ellipse, we have the following constructive conditions for all nanoslits:

$$-\varphi + \psi(O, F_1) + 2\pi r_1 / \lambda_{\text{spp}} = 2\pi m + \varphi_1 \quad (\text{S1})$$

for $|\sigma_-\rangle$ illumination at point F_1 , and

$$\varphi + \psi(O, F_2) + 2\pi r_2 / \lambda_{\text{spp}} = 2\pi n + \varphi_2 \quad (\text{S2})$$

for $|\sigma_+\rangle$ illumination at point F_2 , where m and n are integers, φ_1 and φ_2 are constant values and λ_{spp} is the SPP wavelength.

By adding the two equations above, we can eliminate the angle φ , and have

$$r_1 + r_2 = \left[m + n - \frac{\psi(O, F_1) + \psi(O, F_2)}{2\pi} + \frac{\varphi_1 + \varphi_2}{2\pi} \right] \lambda_{\text{spp}} \quad (\text{S3})$$

Because $\psi(O, F)$ is either 0 or π , the third term on the right side in the bracket of Eq. S3 is either 0, 0.5 or 1. So we can rewrite the above equation as follows:

$$r_1 + r_2 = (k / 2 + \varphi_0) \lambda_{\text{spp}} \quad (\text{S4})$$

where k is an integer, and $\varphi_0 = \frac{\varphi_1 + \varphi_2}{2\pi}$.

If we assume that only photons with one certain spin state can be accumulated at point F_1 and point F_1 simultaneously. Take the photons with $|\sigma_-\rangle$ spin state for example, we have:

$$-\varphi + \psi(O, F_1) + 2\pi r_1 / \lambda_{\text{spp}} = 2\pi m + \varphi_1 \quad (\text{S5})$$

at point F_1 , and

$$-\varphi + \psi(O, F_2) + 2\pi r_2 / \lambda_{\text{spp}} = 2\pi n + \varphi_2 \quad (\text{S6})$$

at point F_2 . By subtracting these two equations from each other, we get an equation that determines the coordinates of nanoslits as follows,

$$r_1 - r_2 = [k / 2 + \varphi_0] \lambda_{spp} \quad (S7)$$

where $\varphi_0 = \frac{\varphi_1 - \varphi_2}{2\pi}$. The above equation indeed shows that the nanoslits are located at hyperbolic trace

with two foci at F_1 and F_2 .

2. Discussion of the focusing of semicircular slit with circular polarization lights

Fig. S1 shows a schematic of semicircular slit. The authors in Ref. [1] states that photons with different spin states can be separated and focused with a shift of $\sim \pm \frac{\lambda}{2\pi}$. We should clarify that the focusing in this paper is approximate and not strict.

For each small segment at slit position with azimuthal angle θ , the geometric phase is $\sigma\theta$, where $\sigma = \pm 1$ corresponds to the incident spin state $|\sigma_{\pm}\rangle$. If there exist a point F where all the segments at the slit can constructively interfere with, for example, $|\sigma_{-}\rangle$ illumination, we have

$$-\theta + 2\pi r / \lambda_{spp} = \text{const.} \quad (S8)$$

The position F and the constant value at the right side can be obtained by choosing any three points at the slit. It can be easily verified that the obtained position of F cannot fulfill the above equation at other points any more.

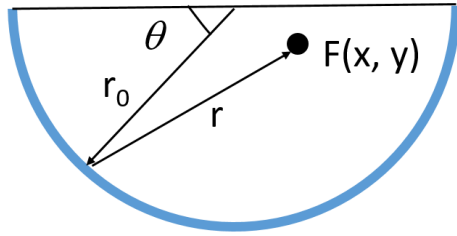


Fig. S1 Schematic of a semicircular slit.

3. The design of metasurfaces, sample fabrication and optical measurements.

For the metasurfaces shown in Figs. 2-3, the locations of foci are designed at F_1 (-2 μm , 0 μm) and F_2 (2 μm , 0 μm), respectively. For the metasurfaces shown in Fig. 4, the foci are F_1 (-5 μm , 0 μm) and F_2 (5 μm , 0 μm), respectively. The geometrical parameters of the nanoslit are identical with width of $w = 50$ nm and length of $L = 200$ nm. The distance between two adjacent nanoslits has a minimum gap of 300 nm to avoid structural overlapping.

We evaporated 100 nm thickness Au film onto a glass substrate and used focused ion beam (FIB) milling to etch the nanoslit structures on the film. The evaporation rate was 0.5 \AA s^{-1} and the beam current was 1.1 pA to ensure the fabrication accuracy. A commercial NSOM system (Nanonics Imaging Multiview 1000) was used to measure the SPP distributions. The probe is metal-coated, tapered fiber probe with about half-cone angle of 15 $^\circ$. The probe was modified with sharp perturbation to increase the coupling efficiency of the \mathbf{E}_z component. In addition, because the \mathbf{E}_z component of SPPs is much larger than the in-plane $\mathbf{E}_{x,y}$ component at the Au surface, the measured optical intensity is expected mostly come from the normal electric field $|\mathbf{E}_z|^2$. The samples were back-illuminated with circular polarized light, which is generated by a quarter wave plate and a polarizer. Figure S2 presents a full schematic of the experimental setup.

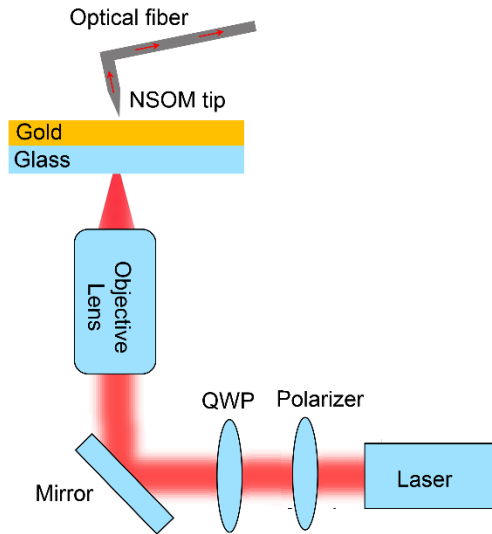


Fig. S2 NSOM setup for measurement of the near field intensity.

4. Simulation results of the metasurfaces shown in Fig. 4

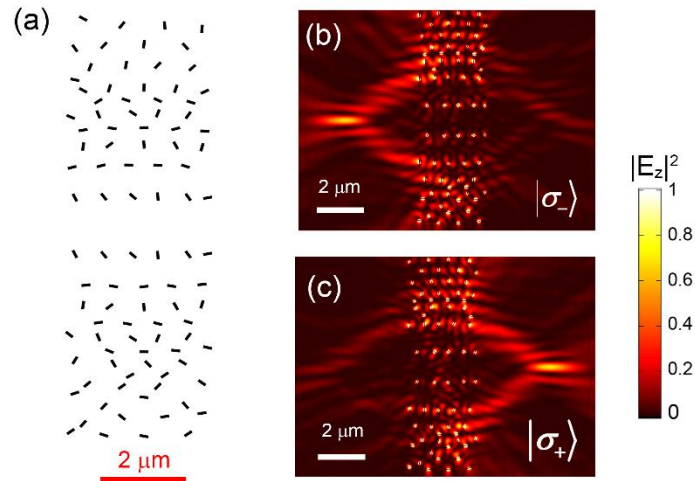


Fig. S3 (a) The design pattern of the metasurface that can focus photons with opposite spin states at each side of it. (b-c) The simulated near-field intensities with $|\sigma_{\pm}\rangle$ illuminations.

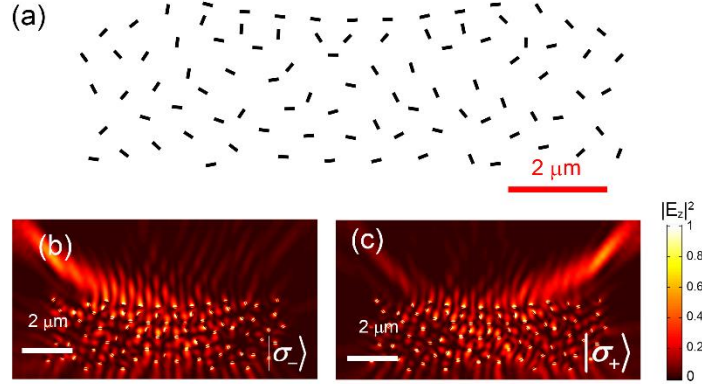


Fig. S4 (a) The design pattern of the metasurface that can focus photons with opposite spin states at the same side of it. (b-c) The simulated near-field intensities with $|\sigma_{\pm}\rangle$ illuminations.

5. Focusing the photons at arbitrary positions relative the metasurfaces

In Fig. 4 of the main text, we have only shown the two cases that the two foci are located at the same side and left-right side. However, the two foci can be located at arbitrary positions relative to the metasurfaces if the proper regions of ellipse-shaped metasurfaces are chosen. In Fig. S5, we have shown other four cases that the two foci can be located at right-down, up-left, up-right and left-down positions relative the square metasurfaces.

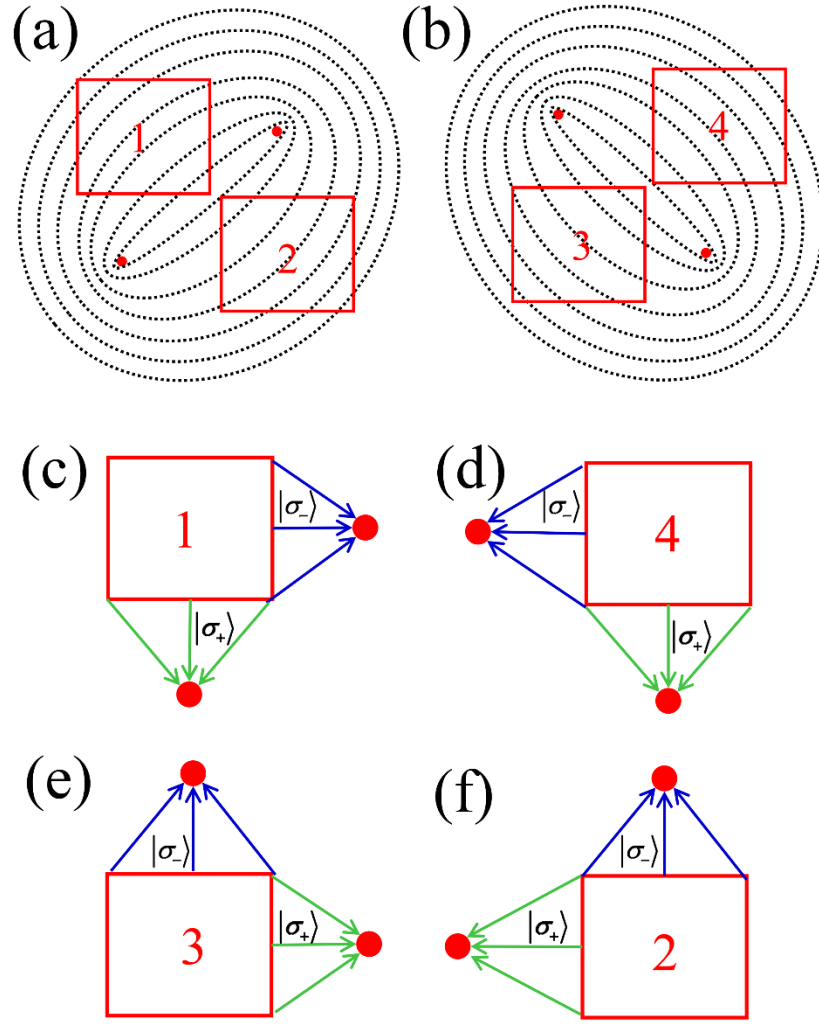


Fig. S5 (a-b) The selecting strategies of the ellipse-shaped metasurface for delivering photons with different spin states at arbitrary positions. (c-f) Schematic of metasurfaces that can focus light with different spin states at right-down, left-down, up-right and up-left positions relative the square metasurfaces.

References:

- [1] K. Y. Bliokh, Y. Gorodetski, V. Kleiner, and E. Hasman, Phys. Rev. Lett. **101**, 030404 (2008).